Influence of bond flexibility on the vapor-liquid phase equilibria of water

Gabriele Raabe[a)]
Institut für Thermodynamik, Technische Universität Braunschweig, Hans-Sommer-Stasse 5, 38106 Braunschweig, Germany

Richard J. Sadus
Centre for Molecular Simulation, Swinburne University of Technology, P.O. Box 218, Hawthorn, Victoria 3122, Australia

(Received 11 October 2006; accepted 5 December 2006; published online 22 January 2007)

The authors performed Gibbs ensemble simulations on the vapor-liquid equilibrium of water to investigate the influence of incorporating intramolecular degrees of freedom in the simple point charge (SPC) water model. Results for vapor pressures, saturation densities, heats of vaporization, and the critical point for two different flexible models are compared with data for the corresponding rigid SPC and SPC/E models. They found that the introduction of internal vibrations, and also their parametrization, has an observable effect on the prediction of the vapor-liquid coexistence curve. The flexible SPC/Fw model, although optimized to describe bulk diffusion and dielectric constants at ambient conditions, gives the best prediction of saturation densities and the critical point of the examined models. © *2007 American Institute of Physics*. [DOI: 10.1063/1.2428302]

I. INTRODUCTION

The phase behavior of either water or aqueous mixtures has a central role in many important biological, chemical, and physical processes. The phase behavior of water has a key role in technical processes such as supercritical fluid oxidation,[1] which provides an environmentally low impact cleaning technology, enhanced oil recovery,[2] and the efficacy of ionic liquids.[3] Although the phase behavior of aqueous systems has been extensively studied experimentally,[4–6] an ability to accurately predict its properties in new situations is of considerable scientific and practical value.

Historically, the traditional approach of developing equations of state[7] has been of limited success for water. Accurate reference equations[8] for pure water have been developed, which cannot be easily extended to mixtures. In contrast, theoretical equations of state can often qualitatively predict[9,10] the properties of aqueous mixtures up to very high pressures but they are not reliable for accurate predictions. In addition, conclusions reached from equation of state calculations are often unclear because of factors such as uncertainties in the theoretical representation of the underlying model and the need to fit equation of state parameters to experimental data.

Molecular simulation[11] provides a useful alternative to equation of state modeling because, when used properly, it provides unambiguous information regarding the merit of the underlying model. There are many alternative models[12] for water, which reflects the difficulty of accurately predicting all the diverse properties of water. Currently, *ab initio* models[13] do not generally provide accurate predictions and the most widely used models are variants of either the four-site[14] (TIP4P) or the three-site simple point charge[15,16] (SPC and SPC/E) models. Extensive investigations of these models indicate that, although they are reasonably accurate at ambient conditions, they show systematic deviations from experiment with increasing temperature. It is only at moderate temperatures that reasonable results can be obtained for saturated liquid densities and vapor pressures.

In an effort to improve the agreement with experiment, more sophisticated models have been developed and tested. Dang *et al.*[17] calculated the vapor-liquid equilibria of water using a polarizable model that included many-body effects,[18] but found only moderate agreement with experiment at higher temperatures. Kiyohara *et al.*[19] compared the vapor-liquid-equilibria (VLE) properties of water predicted by several polarizable models. Quantitative agreement with experimental VLE properties was not obtained at elevated temperatures. Mackie *et al.*[13] reported that a new *ab initio* model underestimated the critical temperature and overestimated vapor pressures.

Other workers[20–23] have endeavored to improve the agreement with experimental phase equilibria data by re-evaluating the parameters of the existing rigid fixed-point charge models[20–22] and/or by replacing[23] the Lennard-Jones potential, which accounts for the dispersive interactions in these models, by the exponential-6 potential. However, it has proved difficult[20,22] to determine a unique set of parameters that can provide simultaneously good descriptions of all VLE properties. Therefore, a model for water that can simultaneously provide a good description of the critical point, vapor pressures, saturation densities, and heat of vaporization of water over a broad range of temperatures remains elusive.

We observe that all previous attempts to optimize fixed-point charge models for the vapor-liquid coexistence curve of water have maintained a rigid, fixed bond separation between the atoms. In contrast, the influence of intramolecular

[a)]Author to whom correspondence should be addressed. Electronic mail: G.Raabe@tu-bs.de

TABLE I. Parameter values for the molecular models examined in this work.

Model	ε_{OO}/k_B (K)	σ_{OO} (Å)	q_O (e)	q_H (e)	$K_{r,OH}/k_B$ (K Å^{-2})	$r_{0,OH}$ (Å)	$K_{\Theta,\angle HOH}/k_B$ (K rad^{-2})	$\Theta_{0,\angle HOH}$ (°)
SPC/E	78.197	3.166	−0.8476	0.4238	∞	1.0	∞	109.47
SPC	78.197	3.166	−0.82	0.41	∞	1.0	∞	109.47
SPC/Ft	78.197	3.166	−0.82	0.41	557 699.5	1.0	46 064.0	109.47
SPC/Fw	78.197	3.166	−0.82	0.41	532 881.6	1.012	3.8 186.5	113.24

vibrations[24–26] has received relatively little attention, as it is commonly believed[27] that molecular vibrations have a minor effect on thermodynamic properties.

The aim of this work is to determine the effect of bond flexibility on the vapor-liquid phase equilibria of water. The phase envelope is calculated using flexible simple point charge water models[28,29] that incorporate intramolecular degrees of freedom and the results are compared with traditional rigid models.

II. THEORY

A. Flexible water models

In the SPC (Ref. 16) model, the oxygen atom is represented as a partially charged Lennard-Jones bead, whereas the hydrogen atoms are simply represented by partial charges without any Lennard-Jones interactions. Water is modeled as a rigid molecule, with the relative positions of the three sites kept constant. The intermolecular interactions are calculated from

$$U_{\text{inter}} = \sum_i \sum_{j<i} \left\{ 4\varepsilon_{ij} \left[\left(\frac{\sigma_{ij}}{r_{ij}} \right)^{12} - \left(\frac{\sigma_{ij}}{r_{ij}} \right)^{6} \right] + \frac{q_i q_j}{r_{ij}} \right\}. \quad (1)$$

In their SPC/Fw model, Wu *et al.*[29] added molecular flexibility to the SPC model by accounting for intramolecular interactions,

$$U_{\text{intra}} = \sum \frac{K_{r,OH}}{2} (r_{OH} - r_{0,OH})^2 + \sum \frac{K_{\Theta,\angle HOH}}{2} (\Theta_{\angle HOH} - \Theta_{0,\angle HOH})^2. \quad (2)$$

The Lennard-Jones parameters and partial charges in the SPC/Fw model remain identical to those used in the SPC model. The force constants (K_r, K_θ) and the equilibrium bond length ($r_{0,OH}$) and angle ($\theta_{0,\angle OH}$) were optimized to reproduce best the experimental bulk diffusion and dielectric constants, but not for the VLE data. The functional form of the SPC/Fw model is identical to the flexible SPC model originally proposed by Teleman *et al.*[28] that we will denote as SPC/Ft. The only difference between the SPC/Fw and SPC/Ft models is in the parametrization of the intramolecular terms.

By comparing simulation results from the flexible models and the corresponding rigid SPC model, we are able to investigate the effect of incorporating intramolecular degrees of freedom, and the influence of their parameterizations on the prediction of the vapor-liquid coexistence curve of water. We also performed simulations on the rigid SPC/E model[15] that uses the same geometry and Lennard-Jones parameters as the SPC model, with the addition of a self-polarization energy correction that slightly increases the partial charges. Thus, our simulations also yield insight into the effect of introducing polarization effects by intramolecular degrees of freedom on one hand, and by increasing the partial charges on the other hand. The parameters used in this work are summarized in Table I.

B. Simulation details

The vapor-liquid coexistence curve of water was calculated via Monte Carlo Gibbs ensemble[30,31] using an existing simulation code,[31] which we modified slightly to include the new model by Wu *et al.*[29] The system consisted of 400 water molecules that were initially equally partitioned in the two simulation boxes. The Ewald sum technique was employed to deal with the electrostatic interactions with a cut-off radius adjusted to half the box length. The cut-off radius for the Lennard-Jones interactions was set to 10 Å, and standard long-range corrections to the energy and pressure were applied. The simulations were equilibrated for 30 000 cycles. The production runs consisted of 60 000 cycles for the fixed models and 100 000 cycles for the flexible models. Longer production runs for the flexible models were required to im-

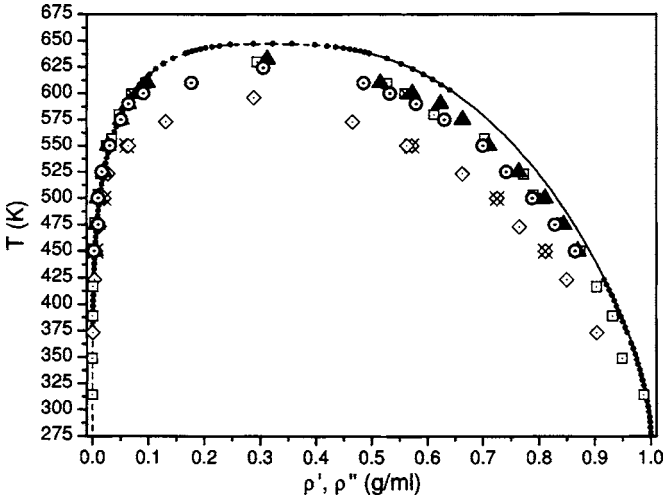

FIG. 1. Coexistence densities of water from Gibbs ensemble Monte Carlo (GEMC) simulation. The squares are the results of SPC/E [(⊡) Boulougouris *et al.*, (Ref. 20); (⊠) this work] and the diamonds show SPC simulation [(◇) Boulougouris *et al.*;⊠ this work]. The results from this work for SPC/Fw are depicted by ▲, and those from SPC/Ft by ⊙. The reference values (Ref. 8) are shown by the solid line, whereas the experimental data by Kell (Ref. 32) and Osborne *et al.* (Ref. 33) are given by ●. Uncertainties of our simulation results are omitted for clarity, but are given in Tables II and III.

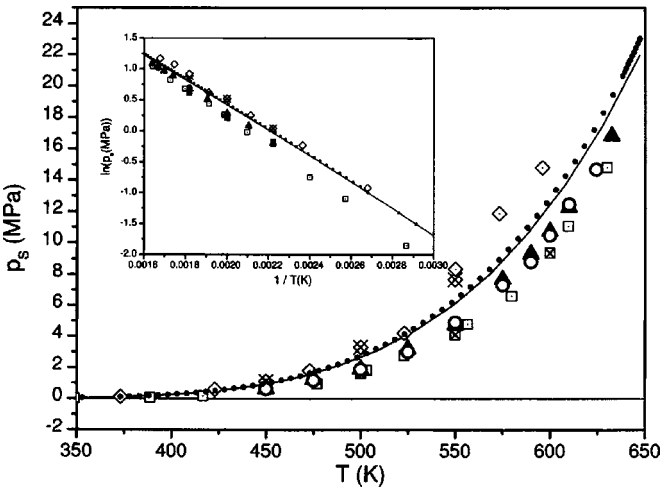

FIG. 2. Vapor pressures from GEMC simulations by flexible and rigid fixed-point charge models for water in comparison with reference data. The squares are the results of SPC/E [(⊡) Boulougouris *et al.*; (⊠) this work] and the diamonds show SPC simulations [(◇) Boulougouris *et al.*; ⧆ this work]. The results from SPC/Fw are depicted by ▲ (this work), and those from SPC/Ft by ⊙ (this work). The reference values (Ref. 8) are shown by the solid line, whereas the experimental data of Osborne *et al.* (Ref. 33) and Stimson (Ref. 34) by small solid circles (●). Uncertainties of our simulation results are omitted for clarity, but are given in Table IV.

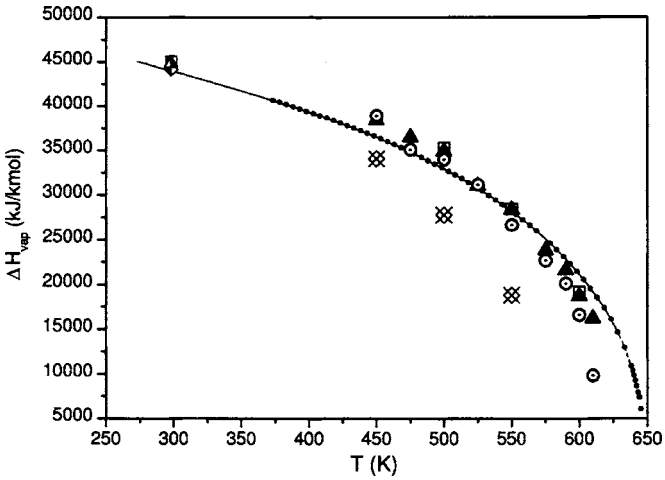

FIG. 3. Comparison between reference data [reference equation (Ref. 8) as solid line, and experimental data (Ref. 33) by ●] for the heat of vaporization for water and Gibbs ensemble simulation results obtained in this work by using the SPC (⧆), SPC/E (⊠), the SPC/Fw (▲), and the SPC/Ft (⊙) water model. Literature data for the heat of vaporization at 298.15 K for SPC, SPC/E, and SPC/Fw (♦, ■, and Δ, respectively) are taken from Wu *et al.* (Ref. 29). Uncertainties of our simulation results are omitted for clarity, but are given in Table V.

prove the statistics because the additional degrees of freedom increased the amount of fluctuations in the simulation. Each cycle consisted of 400 attempted moves, such as a volume change, translation of the center of mass, rotation about the center of mass, and configurational-bias exchanges between the boxes. The moves were selected at random with a fixed probability. However, the probabilities of the different moves were manually adjusted for each temperature to ensure that the equilibrium conditions were satisfied and to avoid empty gas boxes at temperatures below 500 K.

The pressures were calculated via the pressure virial equation. The heats of vaporization (ΔH_{vap}) were determined using the energy (E) and density (ρ) of the liquid and vapor phases and the vapor pressure (p_s),

$$\Delta H_{\mathrm{vap}} = E'' - E' + p_s''\left(\frac{1}{\rho''} - \frac{1}{\rho'}\right). \tag{3}$$

For the flexible models, we also determined the radius of gyration (R_G) along the vapor-liquid coexistence curve to characterize the size of the molecules and its interplay with the thermodynamic properties,

$$\langle R_G^2 \rangle = \frac{\left\langle \sum m_i r_i^2 \right\rangle}{\sum m_i}. \tag{4}$$

Standard deviations of all ensemble averages were determined by dividing the production runs into ten blocks.

The critical properties of the flexible models were estimated by fitting the simulation results at subcritical conditions to the scaling law

$$\rho' - \rho'' = A\tau^{\beta} \quad \text{with } \tau = 1 - \frac{T}{T_C}, \tag{5}$$

and the law of rectilinear diameters

TABLE II. Gibbs ensemble Monte Carlo simulations for the saturated liquid densities (ρ'): comparison of rigid and flexible fixed-point charge models with reference data (Ref. 8). The values in parentheses denote standard deviations.

		SPC/Fw		SPC/Ft		SPC/E		SPC	
T (K)	Reference data ρ' (g/ml)	Simulation (g/ml)	RD (%)	Simulation (g/ml)	RD (%)	Simulation (g/ml)	RD (%)	Simulation (g/ml)	RD (%)
450	0.891 41	0.875 (0.007)	−2	0.865 (0.007)	−3	0.868 (0.005)	−3	0.812 (0.011)	−9
475	0.863 52	0.845 (0.007)	−2	0.829 (0.009)	−4				
500	0.832 32	0.811 (0.006)	−3	0.788 (0.005)	−5	0.794 (0.007)	−5	0.727 (0.012)	−13
525	0.797 09	0.764 (0.010)	−4	0.742 (0.007)	−7				
550	0.756 72	0.710 (0.002)	−6	0.700 (0.008)	−7	0.701 (0.013)	−7	0.572 (0.020)	−24
575	0.709 16	0.664 (0.006)	−6	0.631 (0.017)	−11			0.447 (0.069)	−37
590	0.675 59	0.624 (0.016)	−8	0.580 (0.018)	−14				
600	0.650 20	0.573 (0.030)	−12	0.533 (0.029)	−18	0.560 (0.024)	−14		
610	0.621 39	0.516 (0.030)	−17	0.486 (0.046)	−22				

TABLE III. Gibbs ensemble Monte Carlo simulations for the saturated vapor densities (ρ''): comparison of rigid and flexible fixed-point charge models with reference data (Ref. 8). The values in parentheses denote standard deviations.

		SPC/Fw		SPC/Ft		SPC/E		SPC	
T (K)	Reference data ρ'' (g/ml)	Simulation (MPa)	RD (%)	Simulation (MPa)	RD (%)	Simulation (MPa)	RD (%)	Simulation (MPa)	RD (%)
450	0.004 82	0.0037 (0.0013)	−23	0.0033 (0.0003)	−32	0.0042 (0.0040)	−13	0.0063 (0.0008)	31
475	0.008 17	0.0077 (0.0045)	−6	0.0107 (0.0146)	31				
500	0.013 21	0.0104 (0.0009)	−21	0.0101 (0.0004)	−24	0.0088 (0.0008)	−33	0.0206 (0.0021)	56
525	0.020 64	0.0200 (0.0081)	−3	0.0166 (0.0007)	−20				
550	0.031 51	0.0278 (0.0023)	−12	0.0312 (0.0032)	−1	0.0249 (0.0021)	−21	0.0611 (0.0088)	94
575	0.047 66	0.0512 (0.0053)	7	0.0507 (0.0053)	6			0.1666 (0.0305)	250
590	0.061 31	0.0640 (0.0064)	4	0.0644 (0.0051)	5				
600	0.072 93	0.0814 (0.0128)	12	0.0911 (0.0127)	25	0.0700 (0.0082)	−4		
610	0.087 47	0.0980 (0.0128)	12	0.1771 (0.0504)	102				

$$\frac{\rho' + \rho''}{2} = \rho_c + B\tau. \tag{6}$$

We assumed that the models obey the Ising exponent $\beta = 0.325$. The critical pressures were estimated by extrapolating the vapor pressure curves using the Clausius-Clapeyron equation.

III. RESULTS AND DISCUSSION

The results for the saturation densities, vapor pressures, and heats of vaporization determined by the different models are compared with the results from a fundamental equation of state for water by Pruß and Wagner[8] and experimental data[32–34] in Figs. 1–3. A standard program[35] was used to determine the water properties given by the Pruß and Wagner reference equation. For a quantitative comparison of the results of the different models, we evaluated their relative deviations (RD) from the reference data at various state points, shown in Tables II–V.

As the vapor-liquid coexistence curve given by both the SPC and the SPC/E model has already been the subject of several studies,[20,23,27,36–38] we only performed simulations at a few state points for the quantitative comparison. For the comparison of the simulated saturation densities and vapor pressures given in Figs. 1 and 2, we supplemented our own simulation results for the SPC and SPC/E model with those from Boulougouris *et al.*[20] and their estimates of the critical point. There is good agreement of our results with the literature simulation data.

A. Effect of increased point charge versus bond flexibility

Figure 1 shows that the SPC model in general gives a quite poor description of the vapor-liquid coexistence curve at elevated temperatures with an increasing underestimation of the liquid densities. The simulation results for the heats of vaporization given by the SPC model in Fig. 3 also exhibit significant deviations from the reference values with increasing temperatures. These deviations are due to the fact that the critical temperature of 593.8–596 K predicted by the SPC model[20,23] (Table VI) is considerably lower than the experimental value of 647.1 K.[35] Although the SPC model gives reasonable results for the vapor pressure of water at moderate temperatures, it tends to overpredict the vapor pressure, and yields large and systematic deviations from the reference pressure at higher temperatures as shown in Fig. 2.

The slight increase of the partial charges on the hydrogen and oxygen sites required by the SPC/E water model has a significant effect on the prediction of the vapor-liquid phase equilibria properties. Thus, the SPC/E model yields a

TABLE IV. Gibbs ensemble Monte Carlo simulations for the vapor pressure (p_s): comparison of rigid and flexible fixed-point charge models with reference data (Ref. 8). The values in parentheses denote standard deviations.

		SPC/Fw		SPC/Ft		SPC/E		SPC	
T (K)	Reference data p_s (MPa)	Simulation (MPa)	RD (%)	Simulation (MPa)	RD (%)	Simulation (MPa)	RD (%)	Simulation (MPa)	RD (%)
450	0.9322	0.637 (0.119)	−32	0.616 (0.066)	−34	0.673 (0.405)	−28	1.102 (0.099)	18
475	1.6160	1.214 (0.166)	−25	1.159 (0.225)	−28				
500	2.6392	1.899 (0.104)	−28	1.867 (0.110)	−29	1.625 (0.159)	−38	3.295 (0.218)	25
525	4.1019	3.203 (0.227)	−22	2.997 (0.125)	−27				
550	6.1172	4.708 (0.335)	−23	4.895 (0.251)	−20	4.102 (0.333)	−33	7.667 (0.522)	25
575	8.8140	7.690 (0.278)	−13	7.312 (0.588)	−17			12.040 (0.624)	37
590	10.8210	9.293 (0.365)	−14	8.798 (0.391)	−19				
600	12.3450	10.747 (0.656)	−13	10.478 (0.709)	−15	9.362 (0.470)	−24		
610	14.0330	12.271 (0.625)	−13	12.451 (0.625)	−11				

TABLE V. Gibbs ensemble Monte Carlo simulations for the heat of vaporization (ΔH_{vap}): comparison of rigid and flexible fixed-point charge models with reference data (Ref. 8). The values in parentheses denote standard deviations.

		SPC/Fw		SPC/Ft		SPC/E		SPC	
T (K)	Reference data ΔH_{vap} (kJ/kmol)	Simulation (kJ/kmol)	RD (%)	Simulation (kJ/kmol)	RD (%)	Simulation (kJ/kmol)	RD (%)	Simulation (kJ/kmol)	RD (%)
450	36 486	39 190 (1029)	7	38 900 (2382)	7	38 640 (4055)	6	34 080 (440)	−7
475	37 814	36 510 (2379)	5	35 080 (4849)	1				
500	32 914	34 870 (374)	6	33 990 (363)	3	35 250 (561)	7	27 760 (754)	−16
525	30 725	31 020 (2201)	1	31 110 (3193)	1				
550	28 155	28 360 (696)	1	26 260 (880)	−5	25 400 (476)	1	18 780 (947)	−33
575	25 052	23 800 (934)	−5	22 650 (564)	−10			8 599 (2753)	−66
590	22 823	21 600 (1139)	−5	20 090 (807)	−12				
600	21 123	18 700 (1134)	−11	16 560 (1045)	−22	19 150 (974)	−9		
610	19 182	16 210 (1309)	−15	9 794 (3051)	−49				

higher critical temperature, saturation liquid densities, and heats of vaporization that are much closer to the reference values, as shown in Figs. 1 and 3, and Tables II and V. However, the introduction of the self-polarization energy correction in the SPC/E model results in a remarkable reduction of the predicted vapor pressures and a large underestimation of the experimental values over the entire temperature range (see Fig. 2, Table IV, and also Refs. 20, 23, and 38).

The influence of introducing intramolecular degrees of freedom is best shown by comparing the simulation results of the SPC/Ft model with those from SPC, because both models use the same parameters for ε, σ, q, and the same equilibrium bond length r_0 and bond angle θ_0. The SPC/Ft model can be considered as the exact flexible analog of the SPC model. The comparisons in Figs. 1 and 3 reveal that the introduction of flexibility in the SPC model has a similar effect on the prediction of the vapor-liquid coexistence curve as the increase of the partial charge sites in the rigid SPC/E model. Thus, SPC/Ft as the exact flexible analogs of the rigid SPC model gives lower vapor densities and higher values for the liquid saturation densities and heats of vaporization, resulting in a better agreement with the reference data. With this, the predictions of SPC/Ft are similar to that of the SPC/E model. However, for all models the results for the vapor densities underlie large fluctuations at temperatures below 525 K, as the gas box tends to be populated only by very few molecules.[38]

TABLE VI. Critical properties predicted by rigid and flexible fixed-point charge models of water.

Model	T_c (K)	p_c (MPa)	ρ_c (g/ml)	Z_c
Expt.[a]	647.1	22.064	0.322	0.229
SPC				
Boulougouris *et al.*[b]	596.0	12.6	0.289	0.158
Errington and Panagiotopoulos[c]	593.8	12.9	0.271	(0.174)
SPC/E				
Boulougouris *et al.*[b]	630.0	14.8	0.295	0.172
Errington and Panagiotopoulos[c]	638.6	13.9	0.273	(0.173)
Guissani and Guillot[d]	640.0	16.0	0.290	0.187
SPC/Ft				
This work	624.4	14.68	0.306	0.166
Mizan *et al.*[e]	604.3	12.65	0.2694	(0.168)
SPC/Fw				
This work	634.5	17.25	0.315	0.187

[a]Reference 35.
[b]Reference 20.
[c]Reference 23.
[d]Reference 27.
[e]Reference 25.

The critical temperature of 624.4 K for the SPC/Ft model determined in this work is approximately 30 K higher than that predicted by the SPC model. The SPC/Ft critical density of 0.306 g/ml is much closer to the experimental value than that obtained for SPC (Table VI). We note that our values of the critical properties for the SPC/Ft model do not agree with the work of Mizan *et al.*[25] A possible explanation for these discrepancies could be due to the fact that Mizan *et al.*[25] did not determine the coexistence curve directly from simulations but instead relied on an equation of state that was fitted to pVT data from molecular dynamics simulations.

Although the results of SPC/Ft for the saturation densities are quite similar to those of the SPC/E model, they differ with respect to the prediction of the vapor pressure. This suggests that the introduction of intramolecular degrees of freedom has an additional effect. The flexibility of the models increases the effective dipole moment in a similar way as the increase in the point charges in the SPC/E models. This causes a reduction of the predicted vapor pressures compared to the rigid SPC model and an underestimation of the reference data. This is consistent with the observations by Barrat and McDonald.[39] However, at elevated temperatures, the flexible models predict clearly higher vapor pressure as the SPC/E model. This is best shown by comparing the simulated vapor pressures of the SPC/E and the flexible models at 550 K where the three models yield nearly identical results

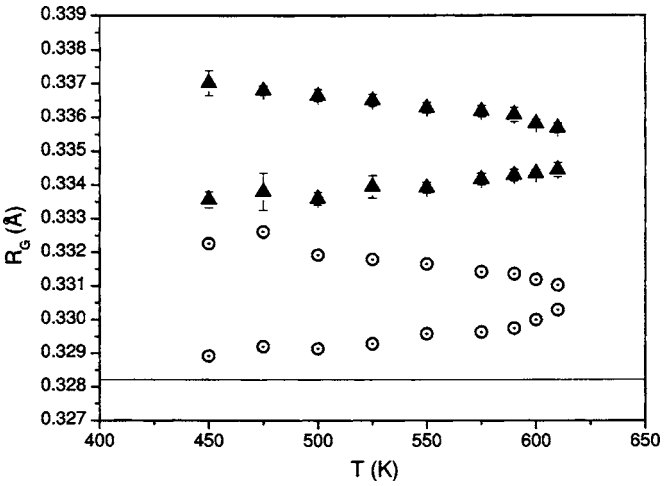

FIG. 4. Radius of gyration R_G along the vapor-liquid coexistence curve for water molecules modeled by SPC/Fw (▲) and SPC/Ft (⊙). The constant R_G=0.328 21 of the rigid SPC and SPC/E models is given as solid line. For both flexible models, the upper branch shows the radius of gyration in the saturated liquid phase, whereas the lower one the value in the vapor phase.

for the liquid density, but the flexible models predict vapor pressures that are by 15%–19% higher than the value of the SPC/E model.

B. Influence of the parametrization of bond flexibility

For the SPC/Fw model, Wu *et al.*[29] used higher values for the equilibrium bond length r_0 and bond angle θ_0 resulting in higher values for the saturation liquid densities, the critical point, and the heats of vaporization than the SPC/Ft model. As illustrated in Fig. 1, the SPC/Fw provides the best prediction of saturation liquid densities of all models examined in this work. The estimated critical temperature of the SPC/Fw water model is 634.5 K, which is only 1.95% below the experimental value, and it is within the range of values reported in the literature for the SPC/E model (see Table VI). The critical density of 0.315 g/ml for the SPC/Fw model is only 2.17% below the experimental value.

The influence of the different parametrization in SPC/Ft and SPC/Fw on the prediction of the vapor pressure is less pronounced. However, the increase in the vapor pressure compared to the SPC/E model means both models give better prediction of vapor pressures above ≈525 K. Therefore, with its higher critical temperature, the SPC/Fw model gives the best estimate of the critical pressure of 17.25 MPa. Although it is substantially below the experimental critical pressure of 22.064 MPa, it nonetheless represents a considerable improvement in accuracy compared with the other models.

C. Radius of gyration

The radius of gyration is a measure of the size of the molecule. Its value for the coexisting liquid and vapor phases at different temperatures is examined in Fig. 4. In a rigid model, such as either the SPC or SPC/E models, the radius of gyration is constant by definition, whereas for the SPC/Fw and SPC/Ft models it can vary depending on the conditions. The values of the radii of gyration for the flexible models are greater than for the rigid model. This was also reported by Wallquist and Teleman.[40] However, the more significant result is that the radii are different in the liquid and vapor phases. As the critical point is approached, the density of the liquid phase decreases and the radius of gyration decreases. Similarly, as the density of the vapor phase increases, the radius of gyration increases. Clearly, at the critical point the radii of gyration of the liquid and vapor phases will attain a common value. Although the absolute difference in value between the phases is small, it arguably more closely reflects the response of a real molecular fluid compared with imposing rigid bonds.

Introducing intramolecular degrees of freedom allows the bond lengths to vary, which means that the effective dipole changes with both temperature and density. For all state points examined in this work, the radius of gyration of the flexible SPC/Ft and SPC/Fw models is higher than the constant value of 0.328 21 Å for the SPC model, resulting in a higher effective dipole moment for the flexible models, although both models use the same parameters for the point charges q_i as SPC. In general, this has a similar effect as increasing the point charges in the SPC/E model. The SPC/Fw model uses larger values for the equilibrium bond length r_0 and bond angle θ_0. This results in higher radii of gyration and therefore higher effective dipole moments along the coexistence curve. Due to this, the SPC/Fw model yields higher values for the saturation liquid densities, the critical point, and the heats of vaporization than the SPC/Ft model, whereas it seems to have less influence on the vapor pressure.

IV. CONCLUSIONS

The introduction of intramolecular degrees of freedom in the SPC/Ft and SPC/Fw models has a similar effect to the increase of the partial charge sites in the rigid SPC/E model. However, at elevated temperatures, the flexible models yield better vapor pressures than the SPC/E model. The flexible SPC/Fw model, although optimized to describe bulk diffusion and dielectric constants at ambient conditions, gives the best prediction of saturation densities and the critical point. The good results for the flexible models are due to the fact that they allow the geometry, and with this the dipole moment, to vary along the coexistence curve.

Historically, efforts in optimizing fixed-point charge models to improve agreement with experimental vapor-liquid phase equilibria have been focused on reevaluating model parameters while maintaining a rigid geometry. In contrast, our results suggest that allowing bond flexibility and optimizing model parameters is a promising alternative strategy for improving the accuracy of phase equilibria calculations.

ACKNOWLEDGMENT

The authors thank the Swinburne Supercomputer Grid for generous allocations of computing time.

[1] S. I. Kawasaki, T. Oe, N. Anjoh, T. Nakamori, A. Suzuki, and K. Arai, Process Saf. Environ. Prot. **84**, 317 (2006).
[2] W. M. Shmonov, R. J. Sadus, and E. U. Franck, J. Phys. Chem. **97**, 9054 (1993).

[3] H. Zhao, Chem. Eng. Commun. **193**, 1660 (2006).
[4] T. M. Seward and E. U. Franck, Ber. Bunsenges. Phys. Chem. **85**, 2 (1985).
[5] M. L. Japas and E. U. Franck, Ber. Bunsenges. Phys. Chem. **89**, 1268 (1985).
[6] E. Brunner, J. Chem. Thermodyn. **22**, 335 (1990).
[7] Y. S. Wei and R. J. Sadus, AIChE J. **46**, 169 (2000).
[8] A. Pruß and W. Wagner, J. Phys. Chem. Ref. Data **31**, 387 (2002).
[9] M. Heilig and E. U. Franck, Ber. Bunsenges. Phys. Chem. **93**, 898 (1989).
[10] N. G. Stetenskaja, R. J. Sadus, and E. U. Franck, J. Phys. Chem. **99**, 4273 (1995).
[11] R. J. Sadus, *Molecular Simulation of Fluids: Theory, Algorithms and Object-Orientation* (Elsevier, Amsterdam, 1999).
[12] A. A. Chialvo and P. T. Cummings, Adv. Chem. Phys. **109**, 115 (1999).
[13] A. D. Mackie, J. Hernandez-Cobos, and L. F. Vega, J. Chem. Phys. **111**, 2103 (1999).
[14] W. L. Jorgensen, J. Chandrasekhar, J. D. Madura, R. W. Impey, and M. L. Klein, J. Chem. Phys. **79**, 926 (1983).
[15] H. J. C. Berendsen, J. R. Grigera, and T. P. Straatsma, J. Phys. Chem. **91**, 6269 (1987).
[16] H. J. C. Berendsen, J. P. M. Postma, W. F. van Gunsteren, and J. Hermans, in *Intermolecular Forces*, edited by B. Pullman (Reidel, Dordrecht, 1981).
[17] L. X. Dang, T.-M. Chang, and A. Z. Panagiotopoulos, J. Chem. Phys. **117**, 2940 (2002).
[18] L. X. Dang and T.-M. Chang, J. Chem. Phys. **106**, 8149 (1997).
[19] K. Kiyohara, K. E. Gubbins, and A. Z. Panagiotopoulos, Mol. Phys. **94**, 803 (1998).
[20] G. C. Boulougouris, I. G. Economou, and D. N. Theodorou, J. Phys. Chem. B **102**, 1029 (1998).
[21] J. L. F. Abascal and C. Vega, J. Chem. Phys. **123**, 234505 (2005).
[22] C. Vega, J. L. F. Abascal, and I. Nezbeda, J. Chem. Phys. **125**, 034503 (2006).
[23] J. R. Errington and A. Z. Panagiotopoulos, J. Phys. Chem. B **102**, 7470 (1998).
[24] C. C. Liew, H. Inomata, and K. Arai, Fluid Phase Equilib. **144**, 287 (1998).
[25] T. I. Mizan, P. E. Savage, and R. M. Ziff, J. Supercrit. Fluids **10**, 119 (1997).
[26] Z. Duan, N. Møller, and J. H. Weare, J. Phys. Chem. B **108**, 20303 (2004).
[27] Y. Guissani and B. Guillot, J. Chem. Phys. **88**, 8221 (1993).
[28] O. Teleman, B. Jönsson, and S. Engström, Mol. Phys. **60**, 193 (1987).
[29] Y. Wu, H. L. Tepper, and G. A. Voth, J. Chem. Phys. **124**, 024503 (2006).
[30] A. Z. Panagiotopoulos, Mol. Phys. **63**, 527 (1987).
[31] http://towhee.sourceforge.net
[32] G. S. Kell, J. Chem. Eng. Data **20**, 97.105 (1975).
[33] N. S. Osborne, H. F. Stimson, and D. C. Ginnings, J. Res. Natl. Bur. Stand. **18**, 389 (1937).
[34] H. F. Stimson, J. Res. Natl. Bur. Stand., Sect. A **73A**, 493 (1969).
[35] E. W. Lemmon, M. O. McLinden, and M. L. Huber, REFPROP, Version 7.0 NIST Standard Reference Database 23.
[36] J. J. de Pablo, J. M. Prausnitz, H. J. Strauch, and P. T. Cumming, J. Chem. Phys. **93**, 7355 (1990).
[37] I. G. Economou, Fluid Phase Equilib. **183–184**, 259 (2001).
[38] J. Vorholz, V. I. Harismiadis, B. Rumpf, A. Z. Panagiotopoulos, and G. Mauerer, Fluid Phase Equilib. **226**, 237 (2004).
[39] J.-L. Barrat and I. R. McDonald, Mol. Phys. **70**, 535 (1990).
[40] A. Wallquist and O. Teleman, Mol. Phys. **74**, 515 (1991).